Binding of XPA and RPA to Damaged DNA Investigated by Fluorescence Anisotropy†

Thomas Hey, Georg Lipps, and Gerhard Krauss*

Lehrstuhl für Biochemie, Universität Bayreuth, Universitätsstrasse 30, 95447 Bayreuth, Germany

Received September 14, 2000; Revised Manuscript Received December 28, 2000

ABSTRACT: The proteins XPA and RPA are assumed to be involved in primary damage recognition of global genome nucleotide excision repair. XPA as well as RPA have been each reported to specifically bind DNA lesions, and ternary complex formation with damaged DNA has also been shown. We employed fluorescence anisotropy measurements to study the DNA-binding properties of XPA and RPA under true equilibrium conditions using damaged DNA probes carrying a terminal fluorescein modification as a reporter. XPA binds with low affinity and in a strongly salt-dependent manner to DNA containing a 1,3-d(GTG) intrastrand adduct of the anticancer drug cisplatin or a 6-nt mismatch (K_D = 400 nM) with 3-fold preference for damaged vs undamaged DNA. At near physiological salt conditions binding is very weak (K_D > 2 μM). RPA binds to damaged DNA probes with dissociation constants in the range of 20 nM and a nearly 15-fold preference over undamaged DNA. The presence of a cisplatin modification weakens the affinity of RPA for single-stranded DNA by more than 1 order of magnitude indicating that binding to the lesion itself is not a driving force in damage recognition. Our fluorescence anisotropy assays also show that the presence of XPA does not enhance the affinity of RPA for damaged DNA although both proteins interact. In contrast, cooperative binding of XPA and RPA is observed in EMSA. Our results point to a damage-sensing function of the XPA−RPA complex with RPA mediating the important DNA contacts.

Nucleotide excision repair (NER)[1] is the major pathway to remove a wide variety of DNA lesions (e.g. UV photoproducts, bulky adducts) throughout all three kingdoms of life (*1*−*3*). In the first step of eukaryotic NER a helix-distorting DNA lesion is bound by an initial damage-sensing activity that recruits further repair proteins to the damaged site. A longer DNA stretch of about 30 nt is then unwound by helicase activity, and structure-specific endonucleases join the repair complex. Double incision of the damaged strand releases 24−32 nt containing the modification. The resulting gap is refilled in a repair synthesis step by DNA polymerase δ or ϵ and sealed by a DNA ligase. The complete system of human NER can be reconstituted from purified (*4*) or recombinantly expressed (*5*) components.

In eukaryotic cells distinct NER pathways for the repair of actively transcribed genes and the removal of damage in the rest of the genome have been identified (*6*). While for both processes a core set of 15−18 proteins seems to be involved in the later steps of NER, clear differences exist with regard to the mechanisms of damage recognition and organization of the pre-incision complex. In transcription-coupled repair RNA polymerase stalled at a DNA lesion is thought to locate the subsequent repair factors including the XPA and RPA proteins to the damaged site. The XPA−RPA complex interacts with other repair factors such as the helicase-containing TFIIH, which is part of the RNA polymerase holoenzyme, and the excision nucleases XPG and ERCC1-XPF.

In global genome repair the nature of the initial damage sensor is still a matter of controversy (*7*). XPA and RPA as well as the XPC−hHR23B complex have been suggested to recognize the DNA lesion, and indeed these proteins have been shown to preferentially bind damaged DNA.

The XPA protein has been considered for a long time to be involved in primary damage recognition. It binds to damaged DNA with a slight preference and modest affinity (*8*−*10*), and it is thought to act in complex with the single-stranded (ss) DNA-binding protein RPA (*11*−*13*).

The heterotrimeric RPA itself is also able to bind different types of DNA lesions (*14*−*16*) and has been implicated in stabilizing the opened DNA duplex in cooperation with XPA, TFIIH, and XPC (*17*). In a recent study a very high affinity of RPA for ssDNA containing damaged sites has been

† These studies were supported by Grant DFG KR 704/10-1 of the Deutsche Forschungsgemeinschaft to G.K., by the Graduiertenkolleg 'Biosynthese der Proteine und Regulation ihrer Aktivität' of the DFG, and by the Fonds der Chemischen Industrie.

* To whom correspondence should be addressed. Phone: +0049-(0)921-552428. Fax: +0049(0)921-552432. E-mail: gerhard.krauss@uni-bayreuth.de.

[1] Abbreviations: RPA, (recombinant) human replication protein A; XPA, XPC, xeroderma pigmentosum group A/C complementing protein; NER, nucleotide excision repair; hHR23B, human homologue of the yeast RAD23 protein; PAGE, polyacrylamide gel electophoresis; EMSA, electrophoretic mobility shift assay; ss, single-stranded; ds, double-stranded; *r*, anisotropy; DTT, dithiothreitol; SDS, sodium dodecyl sulfate; nt, nucleotide; bp, base pair; R, purine nucleotide; Y, pyrimidine nucleotide; UV, ultraviolet light; PT-DNA, DNA containing a cisplatin adduct; (6-4)-product, pyrimidine(6-4)pyrimidone photoproduct; NAAF, *N*-acetyl-2-aminofluorene.

10.1021/bi002166i CCC: $20.00
Published on Web 02/03/2001

reported, suggesting a function for RPA in further unwinding of the damaged site (*18*).

On the other hand increasing evidence suggests that in global genome repair the XPC−hHR23B complex makes an essential contribution to primary damage recognition. On the basis of kinetic repair assays, footprinting, and affinity and specificity measurements employing nonequilibrium methods such as EMSA (electrophoretic mobility shift assay) or coprecipitation (*19*, *20*) XPC has been ascribed the function of the primary damage sensor. The damage recognition problem is still a controversial issue. Both candidates XPA−RPA and XPC−HHR23B have been shown to act first at a damaged site using kinetic in vitro repair assays (*10*, *20*). No clear picture could be obtained when the affinity and specificity for damaged DNA was investigated in DNA-binding assays. However, none of the methods used so far in these studies is a true equilibrium method.

In the present study we applied a sensitive fluorescence depolarization assay to investigate complex formation between damaged DNA and XPA, RPA, or the XPA−RPA complex under true equilibrium conditions.

When small fluorophores are excited by linearly polarized light, the emitted light is depolarized since the molecules rotate and tumble rapidly during the lifetime of the excited state. When the rotational mobility of a fluorescent molecule is decreased, e.g. by complex formation, a lower depolarization or increased fluorescence anisotropy results. In this study we used DNA substrates which had a fluorescein moiety coupled to the 3′-end of one strand. The fluorophore is far away from the damage and supposedly does not interact with protein binding. Furthermore fluorescence can be excited and observed at wavelengths far away from absorption of protein or DNA.

On the basis of this assay, we report quantitative data on the binding of the repair proteins XPA and RPA to 36-bp fluorescent probes bearing helix-distorting sites such as UV photoproducts, mismatched regions, or a single 1,3-intrastrand cisplatin adduct. XPA binds these probes with low affinity and specificity in a strongly salt-dependent manner, while RPA displays high-affinity binding with dissociation constants in the low-nanomolar range and a far higher discrimination between damaged and undamaged substrates as compared to XPA. In binding reactions containing XPA, RPA, and the fluorescent DNA, the formation of a ternary complex can be observed with the fluorescence anisotropy assay.

MATERIALS AND METHODS

Preparation of Proteins. RPA was expressed in *E. coli* BL21 (DE3) using the expression vector pET11d-thRPA (a generous gift from M. S. Wold) and purified following the protocol of Henricksen et al. (*21*) through Affigel-Blue (Biorad), hydroxylapatite (Biorad), and anion-exchange chromatography on EMD-TMAE (Merck, Darmstadt, Germany). RPA eluted from EMD-TMAE at 200 mM KCl at >95% purity as judged by SDS−PAGE and staining with Coomassie Blue. Aliquots containing 10% glycerol were shock-frozen in liquid nitrogen and stored at −78 °C until use.

For a quantitative determination of the DNA-binding activity of our RPA preparation, stoichiometric fluorescence titrations of RPA and ssDNA were performed. ssDNA at a concentration of 50 nM was titrated with RPA in the absence of salt, and the fraction of active protein was determined from the equivalence point of the titration curve.

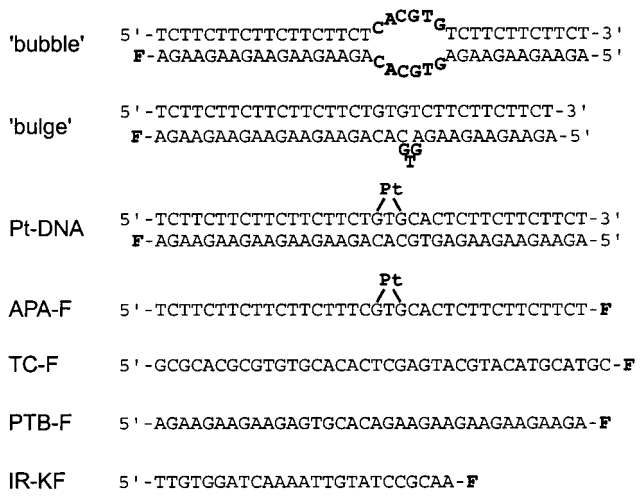

FIGURE 1: Fluorescent DNA probes used to assay XPA and RPA binding. **F** indicates a fluorescein modification attached via a C5-linker. Deviations from normal helix geometry are displayed in bold letters. 'Bubble': 36-nt duplex DNA containing 6 mismatched bases. 'Bulge': 33-nt duplex DNA containing 3 additional bases in one strand. Pt-DNA: 36-bp probe containing a 1,3-d(GTG) intrastrand adduct of cisplatin (**Pt**); the same duplex in its unplatinated form was used as undamaged DNA control in this study. Single-stranded probes were either pyrimidine-rich with or without cisplatin modification (APA-F) or had a mixed (TC-F, IR-KF) or purine-rich (PTB-F) composition.

XPA was expressed as His-tagged protein in *E. coli* BL21 (DE3) pLysS using the plasmid pET15b-XPAC (*8*) (generously provided by R. Wood) and purified by metal chelate chromatography using Ni-NTA fast-flow Sepharose (Qiagen) as described (*22*).

Preparation of DNA with a Single 1,3-Intrastrand d(GTG) Cisplatin Adduct (Pt-DNA). Oligodeoxynucleotides with or without fluorescein modification were purchased from Eurogentech (Seraing, Belgium) in PAGE-purified quality. Oligodeoxynucleotides of the APA series (Figure 1) were allowed to react with a 3-fold molar excess of cisplatin (Sigma) in platination buffer (1 mM sodium phosphate, 3 mM NaCl, pH 7.5) for 24 h in the dark as described (*23*). Platination was stopped by the addition of 0.5 M NaCl and the DNA desalted by G25 spin chromatography (Pharmacia). After 5′-labeling with T4 polynucleotide kinase (NEB) and [γ-^{32}P]ATP (5000 Ci/mmol; Hartmann Analytics, Braunschweig, Germany) the degree of platination was determined by denaturing electrophoresis on 20% polyacrylamide gels (TBE: 89 mM Tris base, 89 mM boric acid, 2 mM EDTA, pH 8.3; acrylamide:bisacrylamide = 19:1) where the platinated oligonucleotide was found to migrate as a single shifted band compared to the unmodified DNA. In all platination reactions not more than 5% interstrand cross-links were present. The complementary strand was added in 10% excess in buffer NEB4 (20 mM Tris·AcOH, 50 mM KOAc, 10 mM $Mg(OAc)_2$, 1 mM DTT, pH 7.9) and annealing was performed by heating the sample to 80 °C for 5 min followed by cooling to room temperature for 2 h. To check the degree of platination the platinated duplex DNA was subjected to analytical restriction by *Apa*LI (NEB), which does not cleave the platinated recognition site, and analyzed by denaturing

PAGE. Reaction products were quantified by electronic autoradiography using an Instant Imager (Canberra Packard). More than 98% of the platinated DNA was found to be resistant against restriction by *Apa*LI.

Electrophoretic Mobility Shift Assays (EMSA). Indicated amounts of RPA and XPA were preincubated in RPA buffer (25 mM HEPES·KOH, 100 mM KCl, 5 mM $MgCl_2$, 1 mM DTT, 100 ng/μL BSA, 0.01% (v/v) Nonidet P40, 0.5% (v/v) inositol, pH 7.8) or XPA buffer (20 mM Tris·Cl, 50 mM NaCl, 1 mM $MgCl_2$, 20 μM $Zn(OAc)_2$, 1 mM DTT, 0.01% (v/v) Nonidet P40, 10% (v/v) glycerol, pH 7.5) for 5 min at room temperature. 2 nM of labeled DNA was added and samples were loaded on native polyacrylamide gels (6%, acrylamide:bisacrylamide = 29:1) after a further 10-min incubation at room temperature. Electrophoresis was carried out in TAE (40 mM Tris-acetate, 1 mM EDTA, pH 8.5) as running buffer for 3 h at 10 V/cm and 4 °C. The gels were analyzed by electronic autoradiography using an Instant Imager (Canberra Packard).

Preparation of Double-Stranded Fluorescent Probes for Depolarization Measurements and EMSA. XPA and RPA are known to bind ssDNA. Therefore it was crucial to keep the amount of ssDNA in the double-stranded probes as low as possible. For this reason the nonfluorescent strand was present in the hybridization reaction in excess over the complementary fluorescent one. Samples of the duplex preparations were tested for their single-strand content by 5′-labeling with T4-PNK and [γ-^{32}P]ATP followed by nondenaturing electrophoresis on 20% polyacrylamide gels (acrylamide:bisacrylamide = 19:1 in TAE (40 mM Tris·AcOH, 1 mM EDTA, pH 8.5) at 10 V/cm for 6 h) and quantization of single-strand content by electronic autoradiography. Only preparations containing less than 5% nonfluorescent ssDNA were used in this study.

To investigate the interaction of the repair proteins with UV-damaged DNA, a duplex of the oligonucleotides APA and PTB-F (Figure 1) was irradiated with UV light at 254 nm. After various irradiation times samples were subjected to fluorescence titration experiments with RPA. Protein binding reached a plateau at dose rates > 10 kJ/m^2 and binding affinities of RPA for UV-damaged DNA were determined for this dosage.

Fluorescence Depolarization Measurements. Free fluorescein in solution displays a rapid rotational motion relative to its fluorescence lifetime. Upon excitation with vertically polarized light the emitted fluorescent light is completely depolarized. Coupling of the chromophore to a larger molecule, e.g. the oligonucleotide probe, reduces its mobility resulting in an increased anisotropy. Upon binding of the fluorescently labeled DNA probe to the repair proteins, the anisotropy of the fluorescein fluorescence is further increased which serves as an indicator of complex formation.

The anisotropy (r) is defined as the difference between the fluorescence intensity emitted parallel and perpendicular ($I_{||}$ and $I_{\perp}$) divided by the total intensity. Fluorescence anisotropies were calculated from fluorescence intensity measurements employing a vertical excitation polarizer and vertical and horizontal emission polarizers according to:

$$r = \frac{I_{||} - I_{\perp}}{I_{||} + 2I_{\perp}}$$

corrected with the experimentally determined grating factor using fluorescein in the appropriate assay buffer as depolarizing sample. The fluorescence anisotropy and the fluorescence intensity of free fluorescein did not change upon addition of XPA or RPA.

All experiments were performed using a LS50B spectrofluorometer (Perkin-Elmer) equipped with a polarization device and a thermostated jacket at 25 °C. Excitation and emission bandwiths were adjusted to 12 and 18 nm, respectively. Fluorescence titrations were performed at an excitation wavelength of 495 nm with a vertical polarizing filter and monitored at an emission wavelength of 525 nm using a 515-nm cutoff filter. Following sample equilibration at least 8 data points with an integration time of 5 s were collected for each titration point.

Fluorescence anisotropy measurements with XPA were carried out in XPA assay buffer (20 mM Tris·Cl, 50 mM NaCl, 2 mM $MgCl_2$, 1 mM DTT, 100 ng/μL BSA, 10 μM $Zn(OAc)_2$, 0.1 mM polyoxydecyl ether (Sigma), 10% (v/v) glycerol, pH 7.5). Measurements with RPA were performed in RPA assay buffer (25 mM HEPES·KOH, 100 mM KCl, 5 mM $MgCl_2$, 1 mM DTT, 100 ng/μL BSA, 0.1 mM polyoxydecyl ether (Sigma), 10% (v/v) glycerol, pH 7.8) except for the titrations of single-stranded substrates where NaCl was added as indicated in the figure legends. The salt addition was necessary to increase the K_D to DNA concentrations where the signal-to-noise ratio was good enough to allow for reliable data collection (typically 0.5−10 nM, depending on the cuvettes used, concentrations are given in the figure legends). Titrations with ssDNA probes were carried out in 10 × 4-mm cuvettes (1 mL) with stirring; dsDNA was titrated in 10 × 2-mm microcuvettes in a sample volume of 150 μL.

Data Processing. Anisotropy mean values were plotted against the protein concentration and fitted using a simple one-site binding model:

$$A + B \rightleftharpoons AB, \text{ with } K = \frac{[A][B]}{[AB]}$$

where [A] represents the concentration of free protein, [B] the free DNA concentration, and [AB] the concentration of the respective protein−DNA complex.

In case of the fluorescence intensities of free and protein-bound DNA probe being the same, the anisotropy was calculated from:

$$r = \frac{[AB]}{[B_0]} r_{AB} + \frac{[B_0] - [AB]}{[B_0]} r_B$$

$$[AB] = \frac{[A_0] + [B_0] + K}{2} - \frac{\sqrt{([A_0] + [B_0] + K)^2 - 4[AB]}}{2}$$

with $[A_0]$ being the total protein concentration, $[B_0]$ the total DNA concentration, r_B the anisotropy of free DNA, and r_{AB} the anisotropy of the protein−DNA complex.

When the total fluorescence intensity changed during the titration experiment, the fractional fluorescence intensities f_B of the free DNA and f_{AB} for the protein−DNA complex

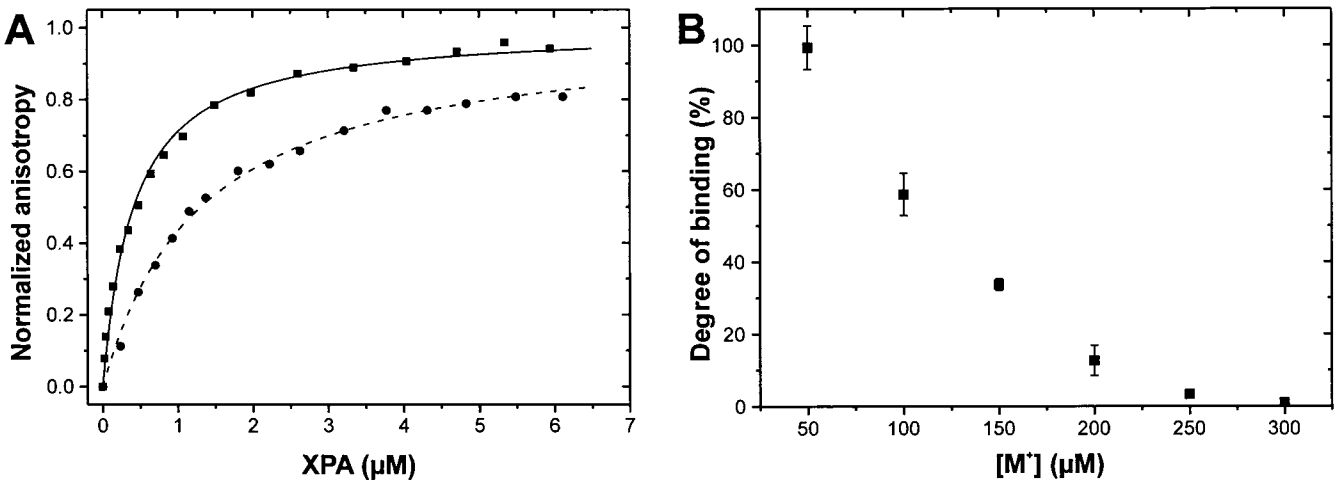

FIGURE 2: Fluorescence anisotropy measurements of XPA binding to DNA. (A) Binding isotherms for the 'bubble' DNA (■) and the corresponding undisturbed probe (●). 10 nM duplex DNA was titrated with XPA in XPA buffer containing 50 mM NaCl/2 mM Mg^{2+}. The normalized anisotropy values representing the degree of binding are given; error bars were omitted for the sake of clarity. (B) Salt dependence of the XPA−DNA interaction. XPA protein was added to Pt-DNA (10 nM in XPA buffer without Mg^{2+}) until anisotropy values showed no further increase (100% binding). The salt concentration was then increased as described in the text keeping the XPA and DNA concentration constant.

had to be considered according to:

$$r = f_{AB}r_{AB} + f_{B}r_{B}$$

$$f_{B} = \frac{([B_0] - [AB])}{([B_0] - [AB]) + [AB]s}$$

$$f_{AB} = \frac{[AB]s}{([B_0] - [AB]) + [AB]s}$$

with *s* representing the intensity ratio of the complexed vs free probe.

Changes in fluorescence intensity might result from interactions between protein and the fluorescein moiety which could influence the strength of complex formation. To check the effect of the fluorescein modification on the binding equilibrium, competition titrations were carried out. In these experiments the single-stranded fluorescent probe alone was titrated with RPA until 80% of DNA was bound. Increasing amounts of unlabeled single-stranded probe were then added until the anisotropy remained constant. The K_D values for both DNA species were calculated from the resulting binding curves. The affinity of RPA for the fluorescein-modified oligonucleotide was found to be up to 30% higher as compared to the unmodified DNA. This small difference is not expected to influence the relative affinities of the repair proteins for the damaged and undamaged DNAs since both carry the same fluorescein modification.

Data sets were least-squares fitted with the program Origin 5.0 (Microcal, Northampton) using the Levenberg−Marquardt algorithm. The curves and data points shown in the figures and tables are based on averaged fits obtained from the recalculation of triplicate measurements. With the exception of one typical titration experiment, the error range for each titration point is omitted from the figures to enhance clarity.

RESULTS

Binding of XPA to Damaged DNA. For a long time XPA has been ascribed the function of the initial damage-sensing protein during NER. XPA has been shown to preferentially bind DNA substrates containing various types of damage such as UV photoproducts, *N*-acetylaminofluorene (NAAF), or cisplatin adducts (*8*, *11*). However, its ability to specifically bind to damaged DNA has not been described in quantitative terms, and the results obtained so far were highly variable, partly due to the methodologies applied. To characterize the DNA-binding properties of XPA under true equilibrium conditions, we applied fluorescence titrations using fluorescence anisotropy as an indicator of complex formation. Oligodeoxynucleotides of 36-bp length bearing a terminal fluorescein modification served as probes in these experiments. The binding of the fluorescent DNA probes to the repair proteins was studied by following the increase in fluorescence anisotropy that results from the formation of large protein−DNA complexes. The complex formation between XPA and damaged DNA was analyzed with duplex DNA substrates carrying either a single 1,3-d(GTG) intrastrand cisplatin adduct, mismatched regions spanning up to 6 nt ('bubble'), or 'bulged' substrates with additional extrahelical bases in one strand (Figure 1).

Figure 2A shows typical binding isotherms for XPA obtained with a mismatched DNA containing a 6-bp 'bubble' and the corresponding completely base-paired probe. As the anisotropy values of both probes differed slightly, the normalized changes in anisotropy are displayed. Upon binding of XPA the anisotropy of the fluorescein-labeled probe increases from 0.1 to 0.16. Analysis of the curves for distorted and undamaged DNA yielded dissociation constants of 380 ± 45 and 1150 ± 84 nM, respectively (Table 1). Titration curves could be well-fitted assuming a one-site binding model. The fluorescence intensities as well as the fluorescence spectra of the DNA probes did not change during the titrations. Titrations with Pt-DNA and the 'bulged' substrate containing three additional bases in one strand yielded similar binding curves and dissociation constants as those obtained for the 'bubble' DNA (Table 1). The anisotropy values were nearly the same: i.e. about 0.10−0.11 for the unbound DNA and 0.16 for the XPA−DNA complex.

Table 1: XPA Binding to Damaged DNA

DNA (see Figure 1)	salt conditions ($NaCl/MgCl_2$)	K_D (nM)
nondamaged	50 mM/2 mM	1150 ± 84
'bubble'	50 mM/2 mM	380 ± 45
'bulge'	50 mM/2 mM	350 ± 49
Pt-DNA	50 mM/2 mM	415 ± 56
	−/−	143 ± 26
	100 mM/−	718 ± 67
	−/5 mM	>2000
ss (R-rich)	50 mM/2 mM	>3000
ss (Y-rich)	50 mM/2 mM	786 ± 98
ss (R/Y-mix)	50 mM/2 mM	355 ± 38

The binding of XPA to damaged DNA has been reported to increase with the degree of helix distortion by the lesion (*9*). The literature data suggested the involvement of partially unpaired bases or short single-stranded regions in damage recognition. In support of this interpretation XPA has been also found to bind ssDNA with affinities comparable to those determined for UV-treated dsDNA fragments (*8*). In our fluorescence depolarization assay XPA also binds to ssDNA with affinities similar to those displayed for double-stranded damaged substrates. Interestingly XPA binding shows a pronounced dependency on the purine/pyrimidine content of the ssDNA probes. It binds with a K_D of 355 ± 38 nM to a sequence consisting of purine/pyrimidine repeats, while a pyrimidine-rich oligonucleotide is bound with one-half this affinity. Purine-rich sequences are very poor substrates for XPA since a plateau could not be reached in these titrations even at protein concentrations up to 5 μM. A fit of these titration curves yielded a $K_D > 3$ μM. For these experiments we used a Tris-buffered solution containing 50 mM NaCl and 2 mM $MgCl_2$. Similar conditions have been used in the binding studies reported in the literature. When XPA binding to DNA was followed in the buffer employed for the RPA titrations (HEPES, 100 mM KCl and 5 mM $MgCl_2$) only very weak binding was observed in fluorescence anisotropy measurements as well as in the EMSA (data not shown). This observation prompted us to study the influence of the ionic strength more closely. Pt-DNA was titrated with XPA in the presence of 50 mM NaCl until anisotropy reached a plateau: i.e. the DNA was completely complexed by XPA. The ionic strength was then increased in steps of 50 mM NaCl by exchanging a part of the sample volume with XPA and DNA in high-salt buffer thereby keeping the concentrations of XPA and DNA constant. As illustrated in Figure 2B the anisotropy decreases significantly upon addition of NaCl and reaches the value of unbound DNA at a 300 mM salt concentration. The change in anisotropy correlates well with the decrease in protein binding in this experiment since the anisotropy of the free DNA probe is not influenced by salt addition in this concentration range. The strong salt dependence is also demonstrated in titration experiments without salt and with 100 mM NaCl added where the dissociation constants differ by a factor of ~5. When the effect of Mg^{2+} ions was assayed in titration experiments, a strong inhibition of XPA binding to damaged as well as undamaged DNA is observed in the presence of Mg^{2+} (see Table 1). At near physiological conditions (5 mM Mg^{2+} and 100 mM KCl) XPA binds platinated DNA only very weakly in our fluorescence-based assay ($K_D > 2$ μM). This low affinity to damaged DNA is not compatible with the proposed function of XPA in primary damage recognition. Furthermore, the 3-fold preference for damaged vs undamaged DNA would allow only a very inefficient detection of damaged sites. Our further studies therefore focused on RPA and the RPA−XPA complex as candidates for damage-sensing.

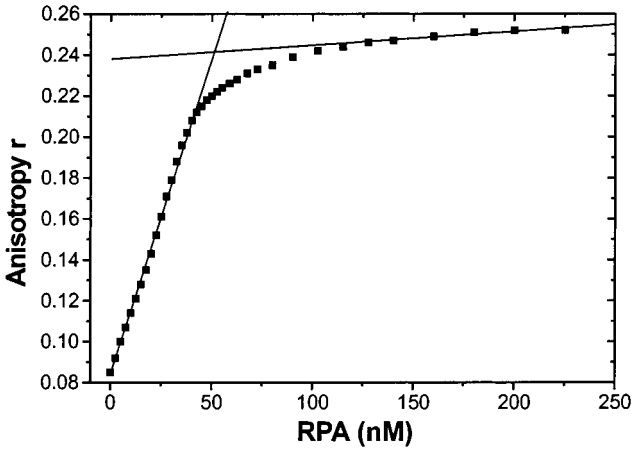

FIGURE 3: Stoichiometric titration of RPA. Anisotropy values are displayed for a 25-nt ssDNA probe (IR-KF, 50 nM in RPA buffer without salt added) upon titration with RPA. The solid lines represent the linear regression curves obtained for 0−30 nM RPA and 100−200 nM RPA; their intersection yields the equivalence point of the titration (~51 nM).

Binding of RPA to Damaged dsDNA. For the RPA binding experiments it was first important to determine the amount of active protein in the RPA preparation. The purification of RPA makes use of an Affigel-Blue chromatographic step during which the protein is eluted under harsh conditions in a buffer containing 1.5 M NaSCN. This highly chaotropic salt may lead to inactivation of the protein (*24*). To test our RPA preparation for the concentration of active protein, we carried out fluorescence titrations with a 25-nt ssDNA probe under stoichiometric binding conditions (Figure 3). RPA displays very high affinity for this substrate with complex dissociation constants in the subnanomolar range. When 50 nM of the single-stranded fluorescent probe were titrated with RPA, the initial anisotropy value of 0.085 increased linearly with the protein addition and reached a plateau value of 0.25. The linear parts of the binding curve were fitted and extrapolated separately, and from the intersection of the lines the protein concentration needed to completely bind the DNA was determined. This equivalence point − together with the known DNA concentration − yielded the active protein concentration in the RPA preparation. More than 95% of RPA protein was active in DNA binding in this assay assuming a 1:1 stoichiometry for binding to the probe, and the activity was stable for at least 6 months. Therefore, in all following experiments, RPA concentrations given represent active protein.

Earlier studies mainly using EMSAs demonstrated specific binding of RPA to dsDNA damaged by UV light or the anticancer drug cisplatin (*14*, *15*). However variable specificity factors for the binding of damaged vs undamaged DNA have been determined from these nonequilibrium methods. To measure true equilibrium binding constants in solution, we carried out fluorescence titrations with the damaged dsDNA substrates shown in Figure 1.

In our titrations RPA binds to duplex DNA substrates containing helix-distorting lesions with high preference as compared to undamaged DNA. The DNA probes bearing

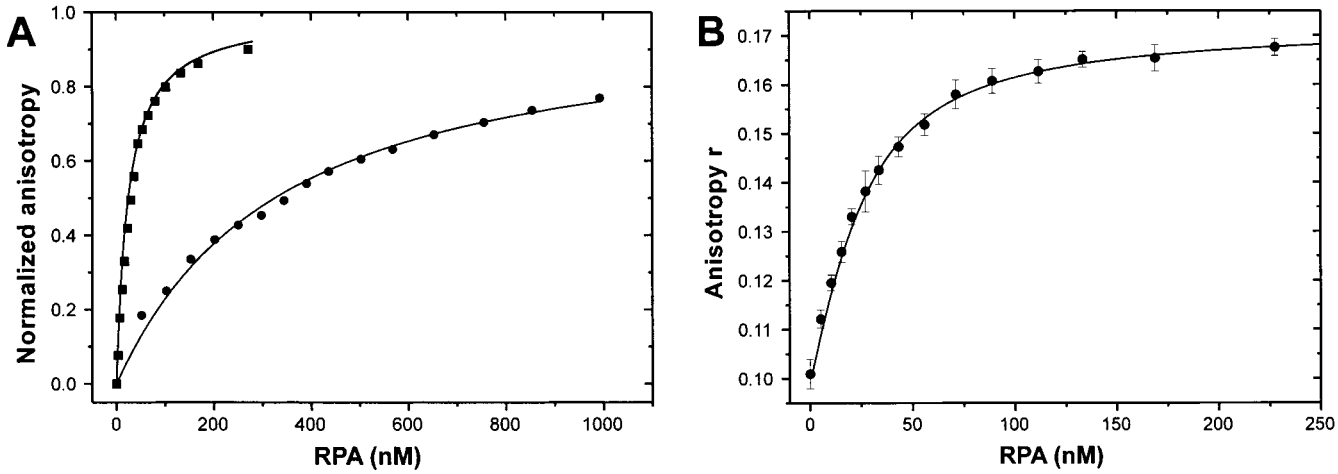

FIGURE 4: RPA binding to damaged DNA. (A) Binding of RPA to the 'bubble' DNA (■) and the corresponding undisturbed probe (●). (B) Binding of RPA to Pt-DNA. Anisotropy values with standard deviations are displayed for a typical fluorescence titration experiment with 10 nM fluorescent DNA probe in RPA buffer. The experiment was performed with 10 nM of duplex DNA in RPA buffer as indicated in the Methods section. The degree of binding was calculated using the anisotropies of the free and complexed DNA obtained from the fit of the binding curves.

Table 2: RPA Binding to Damaged DNA

DNA (see Figure 1)	specificity factor[a]	K_D (nM)
nondamaged	1	245 ± 36
'bubble'	15	16 ± 3
'bulge'	2	~150[b]
Pt-DNA	11	23 ± 5
Pt-DNA−XPA[c]	10	25 ± 6
UV-damaged[d]	8	31 ± 4
	salt added	
ss (R-rich)	1.35 M	77[e]
ss (Y-rich)	1.35 M	4.4 ± 0.4
ss (Y-rich)	0.85 M	0.6[f]
ssPT-DNA (Y-rich)	0.85 M	11 ± 2

[a] Ratio of K_D values for undamaged/damaged DNA. [b] Poor fit, estimated value. [c] See Figure 6. [d] No specific photoproduct. [e] Single measurement only. [f] Extrapolated from Figure 5B.

cisplatin adducts or a disturbed double-helical structure due to mismatched regions ('bubbles') are bound with specificity factors of up to 15. Figure 4 shows typical binding curves obtained with these substrates. These data could be fitted using a one-site binding model. At RPA concentrations above 500 nM, a further small linear increase of anisotropy is observed which is probably due to multiple RPA binding (data not shown). This low-affinity phase of the binding curve was not considered in the calculation of the binding constants.

Fitting of binding curves for the 'bubble' substrate containing a 6-bp mismatch yields a K_D of 16 ± 3 nM, indicating at least 15-fold stronger binding as compared to the undisturbed DNA (245 ± 36 nM). The DNA probe bearing a single cisplatin 1,3-d(GTG) intrastrand adduct was bound with an affinity of 23 ± 5 nM which is comparable to the 'bubble' substrate, while for the heavily UV-irradiated probe containing multiple photoproducts a slightly higher K_D of 31 ± 4 nM was determined (Table 2). The 'bulged' DNA is bound with an affinity between those observed for the 'bubble' and the undamaged DNA. In this case the fit was rather poor and only estimates can be given for the K_D value. In comparison, XPA binds with similar affinities to the 'bulge', the 'bubble', and the platinated DNA. RPA might require partially single-stranded regions or stronger helix distortions for efficient binding of damaged DNA than those caused by the additional extrahelical bases in our 'bulged' DNA probe.

In studying the binding of RPA to dsDNA the general strand-unwinding activity reported for this protein has to be considered. Turchi et al. postulated that RPA binding to damaged DNA might occur via denaturation of the DNA duplex with concomitant binding of the resulting single strands (*25*). We therefore tested for the presence of ssDNA in our binding reactions using the same methodology as these authors. Solutions containing RPA and radioactively labeled double-stranded probes were treated with SDS and proteinase K and then subjected to nondenaturing PAGE. After a 30-min incubation with RPA, not more than 10% of the DNA probe was present in single-stranded form which indicates a low extent of denaturation of the damaged DNA duplex and confirms the specificity of RPA binding to damaged duplex DNA. The presence of 5 mM $MgCl_2$ and the elevated ionic strength in our assays apparently inhibit the unwinding activity displayed by RPA under low-salt conditions (*26*).

Binding of RPA to Damaged ssDNA. The binding of RPA to damaged dsDNA has been often explained in terms of a destabilization of base pairing in the vicinity of a DNA lesion allowing stable binding of RPA to the single-stranded regions. However specific binding of RPA to damaged ssDNA has recently been reported (*18*). In this study the complex formation between RPA and a single-stranded 49-nt oligonucleotide containing various specific UV photoproducts was followed by EMSA, and a very strong and preferential binding to damaged vs undamaged ssDNA was observed. Dissociation constants were extremely low (down to 3 pM), and binding must have been stoichiometric in many of these experiments. As RPA has been repeatedly reported to preferentially bind cisplatin-damaged dsDNA with affinities comparable to UV-damaged probes, we followed RPA binding to ssDNA containing a single 1,3-d(GTG) intrastrand cisplatin adduct.

The RPA−ssDNA interaction is very strong with complex dissociation constants in the subnanomolar range. Although the anisotropy assay is very sensitive, the lower limit of fluorescein-labeled DNA probes that can be reliably mea-

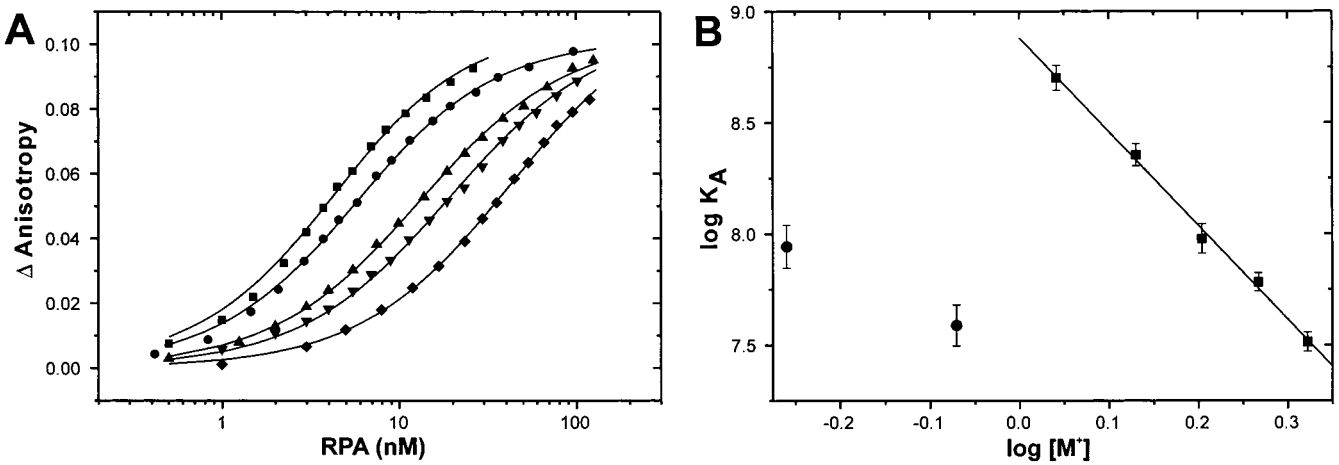

FIGURE 5: Salt dependence of the single-strand binding activity of RPA. (A) Binding isotherms for the RPA interaction with the unmodified oligonucleotide APA-F (1 nM) measured in RPA buffer supplemented with 1 (■), 1.25 (●), 1.5 (▲), 1.75 (▼), and 2 M (◆) NaCl. (B) K_A values as determined from the data shown in panel A are plotted as log K_A vs log [M^+] (■). Data obtained for the platinated single strand at 0.6 and 0.85 M salt are indicated by ●. The binding of RPA to the single-stranded Pt-DNA is 1−2 orders of magnitude weaker as compared to the undamaged probe.

sured is in the concentration range of 0.5 nM with our optical setup. We therefore studied the interaction between RPA and the single-stranded probes under high-salt conditions. Salt was added until the K_D values were in the low-nanomolar range. For titrations of 0.5 nM of the pyrimidine-rich undamaged ssDNA probe, addition of at least 1 M NaCl to the assay buffer was necessary to obtain binding curves from which binding constants could be derived. Stoichiometric titrations under high-salt conditions yielded a 1:1 stoichiometry, as did the low-salt measurements (see above), and showed that more than 90% of the RPA preparation was active even in the presence of 1 M NaCl. With the ssDNA as a substrate the total fluorescence intensity decreased during the titration indicating a change in the environment of the fluorescent dye upon complex formation. This change in intensity has been considered in the evaluation of the binding parameters as described in the Methods section. To investigate the influence of the fluorescein residue on protein binding, competition titrations were carried out (data not shown, see Materials and Methods).

The titration of the cisplatin-modified single-stranded oligodeoxynucleotides which contained at least 95% cisplatin modification with less than 5% interstrand adducts indicated that these probes are bound with significantly lower affinity than the unmodified ones. Quantitative analysis of binding could therefore be performed at salt concentrations below 1 M NaCl, and K_D values were determined in the presence of 0.6 and 0.85 M salt. To compare the data obtained at different salt concentrations, we made use of a general relation between salt concentration and stability of protein−ssDNA complexes (*27*). According to Record and co-workers a linear relationship is observed in double-logarithmic plots of the dissociation constants of protein−DNA complexes against the salt concentration (*28*). Figure 5 shows the dependence of the complex formation between RPA and undamaged ssDNA on the NaCl concentration in a salt range from 1 to 2 M. Assuming a linear relationship also in the range between 0.5 and 1 M salt, binding affinities for the undamaged DNA were extrapolated to the salt conditions present in the titrations with platinated ssDNA. At 0.85 M salt the K_D for the unmodified DNA is extrapolated to be 0.6 nM which is more than 1 order of magnitude lower than the K_D value measured at this salt concentration for the cisplatin-modified strand (Table 2). Clearly, the presence of the cisplatin modification weakens binding of RPA to ssDNA significantly. Lao et al. found the opposite effect: an affinity enhancement of 2 orders of magnitude for the interaction between RPA and ssDNA containing a UV photoproduct (*18*). Obviously the presence of the cisplatin adduct leads to a distinct change of the ssDNA structure and a loss in conformational flexibility. A high flexibility might be a prerequisite for strong interaction with the ssDNA binding domains of RPA.

Complex Formation between XPA, RPA, and Damaged DNA. In the initial steps of NER the proteins XPA and RPA are thought to interact with each other in a cooperative manner. XPA−RPA interaction on DNA has been shown in vitro by pull-down assays and supershifting in EMSA (*11*, *29*), and the formation of the binary XPA−RPA complex has been quantitatively analyzed using the surface plasmon resonance technique (*13*). By fluorescence anisotropy we also could follow the ternary complex formation between XPA, RPA, and damaged DNA. A titration of cisplatin-modified dsDNA with increasing concentrations of the XPA−RPA complex is shown in Figure 6. To ensure formation of the XPA−RPA complex, a 4-fold excess of XPA over RPA was used in these experiments. Recombinantly expressed XPA is known to have folding problems, and the large excess of XPA was intended to account for the partially inactive protein preparation. It was not possible to determine the specific activity of XPA by a fluorescence titration under stoichiometric conditions due to the low binding affinities XPA displays for our damaged DNA probes. The excess of XPA did not interfere with the RPA−DNA titration since XPA alone binds only very weakly to this DNA probe under the salt conditions used in the assay (see above). RPA alone binds tightly to the cisplatin-damaged DNA probe, and extrapolation of the anisotropy for the complex yields a value of 0.18. Unexpectedly, the presence of XPA had no effect on the binding affinity of RPA. When the damaged DNA was titrated with the preformed XPA−RPA complex, the anisotropy values at saturation (1300 nM XPA, 350 nM RPA) were clearly higher than for RPA alone (0.195 vs 0.18). However, the K_D values evaluated from the binding curves

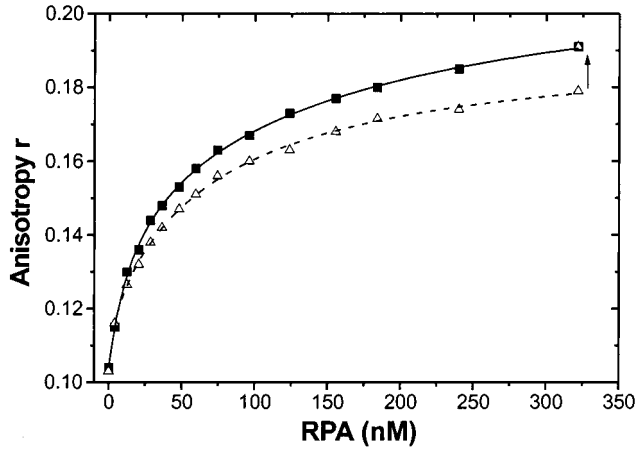

FIGURE 6: Ternary complex formation between RPA, XPA, and Pt-DNA followed by fluorescence anisotropy. Pt-DNA (10 nM) in RPA buffer was titrated with RPA alone (△) or a pre-formed XPA−RPA complex (XPA:RPA = 4:1; ■). The arrow (↑) indicates the anisotropy increase in the RPA alone titration upon addition of XPA yielding a final concentration of 200 nM in the assay (see text for details).

are the same indicating that there is no cooperativity in the formation of the ternary complex. In a further experiment the damaged DNA probe was titrated with RPA alone until saturation and XPA was then added to a final concentration of 200 nM. Thereby the anisotropy increased to the value observed in the titration of the XPA−RPA complex and remained constant upon further addition of XPA. This observation indicates that the effect is based on a specific interaction of the two proteins and is not due to additional XPA binding to DNA since the total XPA concentration differs significantly in both types of experiment (1300 vs 200 nM). When binding to the fluorescent DNA probe is assayed in EMSA a different result is obtained. In the bandshift assay XPA addition to the RPA−DNA complex leads to a strong increase in the degree of DNA binding in a dose-dependent manner over the concentration range of RPA used in the fluorescence titration. Furthermore, the apparent binding affinities determined from EMSA are significantly weaker as those obtained from the fluorescence titrations, and addition of a larger excess of XPA is necessary (data not shown; see also ref *29*). This observation indicates a bias of the affinities determined due to the methodology applied. We do not have a feasible explanation for these effects yet.

DISCUSSION

Damage recognition is a crucial step in NER since the proteins involved have to bind a broad spectrum of DNA lesions with high affinity and preference over undamaged sites. At present the XPC−hHR23B or XPA−RPA complex has been implicated in this function during global genome repair. However, conflicting data were obtained when the binding affinity and specificity for damaged DNA were determined for these proteins. In the present work fluorescence anisotropy has been used as a tool to study the interaction between the NER proteins XPA and RPA − either alone or in a binary complex − and damaged DNA probes. The change in anisotropy of fluorescein-labeled damaged oligodeoxynucleotides upon binding to the repair proteins enabled us to determine the affinity of XPA and RPA to damaged DNA under true equilibrium conditions.

XPA has long been a prime candidate for damage recognition since it was the first NER component identified that displayed preferential binding to DNA containing various types of damage such as UV photoproducts, NAAF, or cisplatin adducts (*8*, *11*). These studies mainly employed EMSA or pull-down assays, and the apparent dissociation constants for binding of XPA to damaged DNA were in the range of 400 nM with an about 3-fold lower affinity for the undamaged control. In the fluorescence anisotropy measurements of the present work, dissociation constants for XPA binding to a 36-bp DNA probe carrying a single 1,3-d(GTG) cisplatin adduct were found to be in the same range. Our measurements also show that XPA binds to single-stranded probes nearly as well as to the damaged probes. A slightly higher dissociation constant for oligonucleotides containing purine−pyrimidine or pyrimidine-rich sequences as compared to damaged DNA − in agreement with the literature (*8*) − is determined from our fluorescence anisotropy assay. Interestingly our measurements indicate a much weaker binding of XPA to purine-rich ssDNA. XPA shares this property with many ssDNA-binding proteins (*24*). Presumably the XPA−ssDNA complex is stabilized by hydrophobic interactions involving π-stacking between aromatic amino acid side chains and the DNA bases which is more efficient with pyrimidine bases. In purine-rich sequences this type of interaction may be unfavorable due to the strong stacking tendency of the bases themselves.

Importantly, our data reveal a strong inhibitory effect of monovalent ions and Mg^{2+} on XPA binding to damaged as well as undamaged DNA. Both for damaged and undamaged DNA the K_D increases nearly 10-fold upon addition of 300 mM salt. A similar effect is observed when the Mg^{2+} concentration is increased to 5 mM. The fluorescence anisotropy data are supported by results obtained from EMSA. Our data thus do not support a prominent role of XPA in primary damage recognition since the binding affinities and specificities determined under near physiological conditions seem to be too weak to contribute significantly to the specificity and efficiency of the NER process. Much higher affinities have been reported in a recent study employing surface plasmon resonance to investigate XPA−DNA interactions (*30*). In the presence of 150 mM NaCl and 2 mM Mg^{2+} K_D values ranging from 13 to 58 nM were determined for the binding of XPA to ssDNA and undamaged DNA, respectively. XPA was found to bind with a K_D of 20 nM to a sensor-chip coupled 70-bp oligonucleotide containing a single (6-4)-photoproduct. A 3-fold weaker binding was reported for the undamaged control. In our study a nearly 20-fold lower affinity was measured for a platinated substrate, although the specificity factors are similar. This discrepancy may be due to the specific features of the surface plasmon resonance experiments or due to a difference in the specific activity of the XPA preparation. The latter is however considered to be unlikely because the protein has been obtained from the same expression system. Unfortunately an assay for measuring the specific activity of XPA is not available.

The human RPA protein interacts with XPA in NER, and it has been found to specifically bind cisplatin-modified DNA (*14*). Complex formation of RPA with DNA containing other

types of damage such as UV photoproducts and NAAF has been also shown (*11*, *15*). Apparent K_D values in the range of 20−200 nM and specificity factors for photodamaged DNA of 2−50 have been reported in these studies. For 1,3-d(GTG) cisplatin adducted DNA a specificity factor of 15 has been determined by EMSA (*25*).

Our fluorescence depolarization measurements yielded K_D values in the range of 15−25 nM for DNA carrying a cisplatin 1,3-intrastrand adduct or an unpaired region of 6 nt. These data are not confounded by inactive RPA molecules since we show by stoichiometric titrations that our RPA preparation is at least 95% active in high-affinity ssDNA-binding. Titrations with UV-irradiated oligonucleotides bearing multiple damaged sites yielded similar affinity constants.

The specificity factor for RPA binding to damaged vs undamaged DNA is determined to be up to 15 with these substrates. A 'bulged' DNA probe containing three extra-helical bases is bound with an affinity intermediate between the undamaged and the 'bubble' or Pt probe. In this case the number of unstacked bases seems to be too small to allow strong RPA binding demonstrating again the positive correlation between the degree of structural deformation and efficient damage recognition by NER proteins.

In a recent work Lao et al. suggested RPA binding to damaged duplex DNA to occur via specific binding to damaged, partially single-stranded sites and further unwinding involving larger single-stranded regions (*18*). This conclusion was based on the much higher affinity of RPA for ssDNA probes containing specific UV photoproducts as compared to undamaged single-stranded probes. On the contrary, our experiments on the binding of RPA to ssDNA reveal a strong inhibitory effect of the presence of the 1,3-intrastrand cisplatin modification on the ssDNA binding activity of RPA. The K_D for the damaged DNA is nearly 2 orders of magnitude higher as compared to the undamaged single-stranded probe. A similar observation has been reported by Patrick et al. who reported a 3-4-fold weaker binding to a single-stranded probe containing the cisplatin 1,2-adduct (*25*). Furthermore these authors describe an inhibition of RPA binding to an 8-bp 'bubble' structure by a cisplatin modification in the single-stranded region. Considering these strongly diverging results for different types of damage, it is unlikely that the high-affinity binding of RPA to the modified single-stranded regions could be the general driving force in the binding of RPA to damaged DNA. It has been also suggested that RPA binding induces complete melting of the dsDNA thereby generating ssDNA for high-affinity binding (*25*). From our electrophoretic analysis of the binding reactions we estimate that not more than 10% of the Pt-DNA probe and 20% of the 'bubble' substrate are present in the single-stranded form following prolonged incubation with RPA. In both cases the amount of protein-bound DNA is significantly higher than the amount of ssDNA indicating a major contribution of duplex-binding events in the RPA-damaged DNA interaction. Similar observations have been reported by Iftode and Borowiec in a study on RPA binding to a 8-bp 'bubble' in the SV40 origin of replication (*31*). These authors concluded that SV40 *ori*-denaturation by RPA occurs in a two-step process with a fast initial binding followed by a slower unwinding reaction. Such a two-step mechanism is believed to be valid also for RPA binding to damaged DNA where formation of an intermediate complex involving RPA in its 8-nt binding mode will take place at sites predestabilized by the helix-distorting lesion (*32*).

The stoichiometry of RPA binding to damaged DNA is not yet clearly resolved. For the damaged dsDNA binding of two molecules of RPA seems to be possible since the damaged as well as the undamaged strand may be complexed. However, our previous photo-cross-linking experiments revealed major contacts between the DNA and the 70-KDa subunit of RPA at the 5′-site of a cisplatin-damaged strand while only minor cross-linking occurred with the undamaged complementary strand (*29*). The titration curves of the present work have been fitted assuming a 1:1 model. The observation of a second weaker binding phase in the titrations with the damaged duplex DNA points to low-affinity binding of further RPA molecules. This is supported by EMSA experiments with the fluorescent probes where the formation of higher-order complexes is observed at high RPA concentrations indicating multiple binding (data not shown).

RPA is known to form a stable complex with XPA, and one should therefore consider a different mode of RPA binding when XPA is present. Cooperative binding of both proteins has been described in earlier studies (*11*), and we obtained a similar result by EMSA where damaged DNA was more efficiently complexed when both XPA and RPA were present (*29*). These EMSA results are in contrast to the fluorescence anisotropy data of the present study on binding of the XPA−RPA complex where we do not observe an influence of XPA on the binding affinity of RPA for platinated duplex DNA. Nevertheless a ternary complex is formed as shown by the increased anisotropy values in the presence of XPA. Interestingly much lower amounts of XPA as compared to those used in EMSA were sufficient to produce this effect which illustrates the large discrepancy of results obtained from the two experimental approaches. Using surface plasmon resonance Wang et al. recently demonstrated ternary complex formation between XPA, RPA, and DNA containing a specific UV photoproduct (*30*). They observed a slightly higher resonance signal response from the DNA-coupled sensor chip after injection of the preformed XPA−RPA complex as compared to the sum of the signals obtained for the separate proteins. This effect has been interpreted in terms of a stabilization of the binding of XPA by an interaction with RPA; a quantitative evaluation was however not given.

From the observation that XPA does not enhance the binding of RPA to damaged DNA under true equilibrium conditions, we conclude that RPA mediates most of the strong contacts of the XPA−RPA complex to the damaged DNA. XPA seems to perform a rather passive function in this in vitro system and contacts the DNA only very weakly. This interpretation is in line with our cross-linking studies on the XPA−RPA complex where only RPA could be cross-linked efficiently to the damaged DNA (*29*).

In summary, we have employed fluorescence depolarization measurements as a sensitive equilibrium method to characterize the binding equilibria between XPA, RPA, and damaged DNA. Our approach allows the determination of binding constants in solution over a wide range of conditions, e.g. the salt concentration. We show a specific but rather weak and highly salt-sensitive interaction of XPA with

damaged DNA, whereas RPA displays strong binding with higher specificity. Our quantitative data show that the RPA−XPA complex rather than XPA alone is the prime candidate for damage recognition during NER. The binding affinity and specificity for damaged DNA of XPA alone is too low to perform this function. In the ternary XPA−RPA−DNA complex most DNA contacts seem to be mediated by RPA. The main function of XPA is probably the recruitment of other repair factors to the damaged DNA site.

DNA lesions occur at low frequency in vivo, and they are removed quite fast and efficiently. The 15-fold preference of the XPA−RPA complex for damaged DNA measured in our in vitro system with purified recombinant proteins and model DNA substrates is certainly not sufficient to account for the specificity of the NER process in vivo. Further proteins or processes seem to be required for efficient damage recognition in the cell.

ACKNOWLEDGMENT

The authors thank M. S. Wold (University of Iowa) and R. Wood (ICRF, South Mimms, U.K.) for the gift of plasmids and G. Boese (MPI für Molekulare Physiologie, Dortmund, Germany) for helpful discussions on the fluorescence depolarization experiments.

REFERENCES

1. Wood, R. D. (1996) *Annu. Rev. Biochem. 65*, 135−167.
2. Ogrunc, M., Becker, D. F., Ragsdale, S. W., and Sancar, A. (1998) *J. Bacteriol. 180*, 5796−5798.
3. Petit, C., and Sancar, A. (1999) *Biochimie 81*, 15−25.
4. Aboussekhra, A., Biggerstaff, M., Shivji, M. K., Vilpo, J. A., Moncollin, V., Podust, V. N., Protic, M., Hubscher, U., Egly, J. M., and Wood, R. D. (1995) *Cell 80*, 859−868.
5. Araujo, S. J., Tirode, F., Coin, F., Pospiech, H., Syvaoja, J. E., Stucki, M., Hubscher, U., Egly, J. M., and Wood, R. D. (2000) *Genes Dev. 14*, 349−359.
6. Bohr, V. A., Smith, C. A., Okumoto, D. S., and Hanawalt, P. C. (1985) *Cell 40*, 359−369.
7. Batty, D. P., and Wood, R. D. (2000) *Gene 241*, 193−204.
8. Jones, C. J., and Wood, R. D. (1993) *Biochemistry 32*, 12096−12104.
9. Buschta-Hedayat, N., Buterin, T., Hess, M. T., Missura, M., and Naegeli, H. (1999) *Proc. Natl. Acad. Sci. U.S.A. 96*, 6090−6095.
10. Wakasugi, M., and Sancar, A. (1999) *J. Biol. Chem. 274*, 18759−18768.
11. He, Z., Henricksen, L. A., Wold, M. S., and Ingles, C. J. (1995) *Nature 374*, 566−569.
12. Matsuda, T., Saijo, M., Kuraoka, I., Kobayashi, T., Nakatsu, Y., Nagai, A., Enjoji, T., Masutani, C., Sugasawa, K., and Hanaoka, F. (1995) *J. Biol. Chem. 270*, 4152−4157.
13. Saijo, M., Kuraoka, I., Masutani, C., Hanaoka, F., and Tanaka, K. (1996) *Nucleic Acids. Res. 24*, 4719−4724.
14. Clugston, C. K., McLaughlin, K., Kenny, M. K., and Brown, R. (1992) *Cancer Res. 52*, 6375−6379.
15. Burns, J. L., Guzder, S. N., Sung, P., Prakash, S., and Prakash, L. (1996) *J. Biol. Chem. 271*, 11607−11610.
16. Patrick, S. M., and Turchi, J. J. (1998) *Biochemistry 37*, 8808−8815.
17. Mu, D., Wakasugi, M., Hsu, D. S., and Sancar, A. (1997) *J. Biol. Chem. 272*, 28971−28979.
18. Lao, Y., Gomes, X. V., Ren, Y., Taylor, J. S., and Wold, M. S. (2000) *Biochemistry 39*, 850−859.
19. Batty, D., Rapic'-Otrin, V., Levine, A. S., and Wood, R. D. (2000) *J. Mol. Biol. 300*, 275−290.
20. Sugasawa, K., Ng, J. M., Masutani, C., Iwai, S., van der Spek, P. J., Eker, A. P., Hanaoka, F., Bootsma, D., and Hoeijmakers, J. H. (1998) *Mol. Cell 2*, 223−232.
21. Henricksen, L. A., Umbricht, C. B., and Wold, M. S. (1994) *J. Biol. Chem. 269*, 11121−11132.
22. Kuraoka, I., Morita, E. H., Saijo, M., Matsuda, T., Morikawa, K., Shirakawa, M., and Tanaka, K. (1996) *Mutat. Res. 362*, 87−95.
23. Moggs, J. G., Yarema, K. J., Essigmann, J. M., and Wood, R. D. (1996) *J. Biol. Chem. 271*, 7177−7186.
24. Kim, C., and Wold, M. S. (1995) *Biochemistry 34*, 2058−2064.
25. Patrick, S. M., and Turchi, J. J. (1999) *J. Biol. Chem. 274*, 14972−14978.
26. Georgaki, A., Strack, B., Podust, V., and Hubscher, U. (1992) *FEBS Lett. 308*, 240−244.
27. Lohman, T. M., and Mascotti, D. P. (1992) *Methods Enzymol. 212*, 400−424.
28. Ha, J. H., Capp, M. W., Hohenwalter, M. D., Baskerville, M., and Record, M. T. J. (1992) *J. Mol. Biol. 228*, 252−264.
29. Schweizer, U., Hey, T., Lipps, G., and Krauss, G. (1999) *Nucleic Acids Res. 27*, 3183−3189.
30. Wang, M., Mahrenholz, A., and Lee, S. H. (2000) *Biochemistry 39*, 6433−6439.
31. Iftode, C., and Borowiec, J. A. (1998) *Nucleic Acids Res. 26*, 5636−5643.
32. Lao, Y., Lee, C. G., and Wold, M. S. (1999) *Biochemistry 38*, 3974−3984.

BI002166I